

## Effect of Cr-doping on the structural,optical and magnetic properties of ZnS nanoparticles prepared by chemical precipitation method

K.Prabaharan<sup>a</sup>, M.Saravanakumar<sup>a</sup>,V.Senthil<sup>c</sup>

<sup>a</sup>Department of Physics, SVS College of Engineering, Coimbatore, India.

---

### ABSTRACT:

ZnS and Cr doped ZnS nanoparticles have been prepared by chemical precipitation method. X-ray diffraction analysis reveals that the undoped and Cr doped ZnS nanoparticles exhibit cubic zincblende structure and the average particle size of the nanoparticles is in the range of 4.8-5.2 nm. The HRTEM studies show that the average particle size of undoped and Cr doped ZnS nanoparticles is in the range of 4.9-5.4 nm. The compositional analysis result indicates that Zn, S and Cr are present in the samples. From the optical studies it is observed that the absorption edge of the prepared ZnS and Cr doped ZnS nanoparticles are shifted towards the short wavelength region (blueshift) when compared to that of bulk ZnS and this shift is due to the quantum confinement effect present in the samples. Photoluminescence studies showed blue emission with appreciable luminescence quenching with increasing Cr concentration. The magnetic behavior of the ZnS nanoparticles with different chromium concentrations has been investigated by magnetism measurements using a vibrating sample magnetometer (VSM). The nanoparticles with lower Cr concentration exhibited strong ferromagnetism, whereas in samples with higher Cr concentration the ferromagnetism was observed to be suppressed.

**KEYWORDS:** Semiconductor nanoparticles, ZnS quantum dots, HRTEM, Quantum confinement effect.

---

### I. INTRODUCTION

Quantum dots of II-VI semiconductors have in particular, received immense attention in recent years because of the ease with which they can be synthesized in the particulate range that leads to quantum confinement. Quantum confinement of electron - hole pair, due to the decrease of the particle size below the Bohr exciton radius, will result in size dependent electronic, optical and magnetic properties, such as increased band gap and the blue shift of absorption edge with decrease of particle size. ZnS is an important semiconductor with a wide band gap of 3.68 eV in bulk form which leads to its wide applications in optoelectronic devices such as solar cells, infrared windows, flat panel displays, sensors and lasers [1-4]. Physical and chemical properties of materials deviate from the bulk properties with the reduction of size of the particles to the nanometer scale. Nanocrystalline ZnS particles have a wide band gap than that of the bulk ZnS. In quantum dot ZnS nanoparticles the optical absorption edge shifts towards the lower wavelength side (blueshift). The increase of band gap with decreasing particle size may be due to quantum size effect [5-8].

Nanocrystalline ZnS has been prepared by different workers using various techniques such as chemical precipitation method, microwave irradiation, micro emulsion, chemical vapor deposition, hot injection, hydro thermal, facile one step method and sol-gel spin coating method [9-16]. Chemical precipitation method is a simple and inexpensive method. Doping of other materials in ZnS nanostructures has gained importance in recent years.

Room Temperature Ferromagnetism (RTFM) in Diluted Magnetic Semiconductor (DMS) materials has been a subject of special interest in view of their potential applications in spintronic

devices. The magnetic properties of DMS are critically dependent on the various semiconductor parameters like the type of semiconductor, mobility and concentration of the charge carriers. For a long period, studies on DMS materials have mainly focused on either bulk materials or thin films. However, the development of future spintronic devices requires DMS materials in reduced dimensionality and size, such as DMS quantum dots. Recent developments in nanotechnology enable the fabrication of low dimension nano-structures of DMS with desired properties. In this direction detailed investigation on tailoring the micro parameters of DMS materials is the need of the day. In the present study Cr (1.99, 2.54 and 3.02 at %) doped ZnS nanoparticles have been prepared by chemical co-precipitation method and the effect of Cr concentration on the morphology, structure, optical and magnetic properties has been discussed.

## II. EXPERIMENTAL

In the present study, Cr-doped ZnS quantum dots have been synthesized through chemical precipitation technique. Aqueous solution of zinc nitrate ( $\text{Zn}(\text{NO}_3)_2 \cdot 6\text{H}_2\text{O}$ ) and required amount of chromium nitrate ( $\text{Cr}(\text{NO}_3)_3 \cdot 9\text{H}_2\text{O}$ ) was stirred for 1h at room temperature. Aqueous solution of sodium sulphide ( $\text{Na}_2\text{S}$ ) was added drop wise to the solution (zinc nitrate + chromium nitrate) and was stirred for 2 hours. A precipitate with yellowish orange color was formed soon after the addition of the  $\text{Na}_2\text{S}$ . The nanoparticles were initially purified by precipitating the particles with excess double distilled water and the solution obtained was centrifuged at 3000 rpm for 10 minutes. The sample was obtained as precipitate and after that the sample was dried at  $150^\circ\text{C}$  for 3 hours.

X-ray diffraction studies have been carried out using PANalytical x-ray diffractometer. Elemental composition of the prepared samples has been studied using Energy dispersive analysis of X-ray (EDAX, Thermo-Noran system Six) and high resolution transmission electron microscope (HRTEM) images of the prepared ZnS and Cr doped ZnS have been recorded using JEOL JEM 2010 microscope. The optical properties have been studied using absorbance spectrum recorded using spectrophotometer (JASCO V-570). Photoluminescence emission spectrum has been recorded using Cary Eclipse spectrophotometer. FTIR studies were carried out using Thermo Scientific Nicolet (iS10). To know the magnetic state of the prepared samples, room temperature magnetization was studied as a function of applied magnetic field in the range of -15,000 to +15,000 G using a Lakeshore Vibrating sample magnetometer, VSM-7410.

## III. RESULTS AND DISCUSSION

Figure 1 shows the X-ray diffraction pattern of ZnS and Cr doped ZnS (1.99% Cr, 2.54% Cr and 3.02% Cr) nanoparticles. The diffraction peaks at  $2\theta$  values  $28.8^\circ$ ,  $48.15^\circ$  and  $56.85^\circ$  are indexed as (111), (220) and (311) planes corresponding to that of cubic zinc blende ZnS. The lattice constants have been found to be  $a=5.3970 \text{ \AA}$  and is in agreement with the standard data of JCPDS card No.03-0570. It is observed that the diffraction peaks of the Cr doped ZnS show a small shift towards higher  $2\theta$  values when compared to that of bulk ZnS. This shift may be due to occupation of Cr ions at the Zn sites. The structural parameters calculated using X-ray diffraction pattern are given in Table 1. The diffraction pattern reveals that the Cr doped ZnS also exhibits cubic zinc blende structure. Doping of Cr in ZnS does not lead to any structural phase transformation but introduces a lattice contraction. The decrease of lattice contraction on Cr doping is because the ionic radius of Cr is less than that of Zn. The average particle size has been calculated using the Scherrer's formulae [17].

$$D = \frac{K\lambda}{\beta \cos\theta} \quad \text{----- (1)}$$

where,  $D$  is the grain size,  $K$  is a constant taken to be 0.94,  $\lambda$  is the wavelength of the x-ray radiation,  $\beta$  is the full width at half maximum and  $\theta$  is the angle of diffraction. The particle size of ZnS and Cr doped ZnS nanoparticles are found to lie in the range 4.8-5.2 nm ( $\pm 0.1 \text{ nm}$ ).

The HRTEM images of the undoped and Cr doped ZnS (1.99% Cr, 2.54% Cr and 3.02% Cr) nanoparticles are shown in Fig. 2. The HRTEM image clearly shows that the undoped and Cr doped ZnS nanoparticles are of nearly spherical in nature. Using the particle number (frequency %) and the average particle diameter of the particles in the HRTEM image the particle size has been calculated. The particle size of undoped ZnS has been obtained as 4.9 nm and the particle size of 1.99% Cr, 2.54% Cr and 3.02% Cr doped ZnS has been found to be 5.1, 5.2 and 5.4 nm respectively. The HRTEM image shown in Fig. 2b, d, f, h exhibit lattice fringes and the lattice spacing has been calculated using these fringes. The interplanar spacing of undoped ZnS is  $3.12 \text{ \AA}$  which corresponds to the (111) plane of the cubic phase of ZnS. HRTEM images of Cr doped ZnS (1.99% Cr, 2.54% Cr and 3.02% Cr) shows lattice fringes with interplanar distance ranging from  $3.10$  to  $3.07 \text{ \AA}$  which also corresponds to the (111) plane corresponding to cubic phase. The lattice spacing of Cr doped ZnS nanoparticles is slightly less than that of undoped ZnS because of the small ionic radius of Cr when compared to that of Zn ( $r_{\text{Cr}^{3+}}=0.63 \text{ \AA}$ ,  $r_{\text{Zn}^{2+}}=0.78 \text{ \AA}$ ). The insets in Fig. 4b, h shows the selected-area diffraction (SAED) patterns of ZnS and 3.02% Cr-doped ZnS. The selected-area diffraction patterns exhibit concentric circles, revealing that the undoped ZnS and Cr doped ZnS are nanocrystalline in nature and are made up of small particles.

Figure 3a-d shows the energy dispersive X-ray analysis (EDAX) of the ZnS and Cr doped ZnS. The chemical constituents present in the sample according to the EDAX results are Zn=51.98% and S=48.02% for undoped ZnS, Zn=50.53%, S=47.48% for 1.99% doped Cr, Zn=50.16%, S=47.30% for 2.54% doped Cr, Zn=49.84%, S=47.14% for 3.02% Cr doped ZnS.

FTIR spectra of ZnS nanoparticles recorded at room temperature in the wavelength range of 4000-400  $\text{cm}^{-1}$  for undoped and Cr doped ZnS nanoparticles are shown in Fig 4a-d. From the spectra the broad band between 3000 and 3700  $\text{cm}^{-1}$  is assigned to O-H stretching vibration of water as characterized by its bending vibration at 1612  $\text{cm}^{-1}$  [18], because all FTIR spectra were recorded by mixing samples with KBr there may be some adsorbed water vapour, as KBr is hygroscopic. The peak at 1375  $\text{cm}^{-1}$  and 1100  $\text{cm}^{-1}$  is assigned to the symmetric bending vibration of methyl group ( $-\text{CH}_3$ ) and C-O group, while the alkenes will have a characteristic C=C stretch at 1600-1680  $\text{cm}^{-1}$  [19]. The peak at 616  $\text{cm}^{-1}$  is assigned to the ZnS band corresponding to sulphides [20].

Room temperature PL spectra of undoped and Cr doped ZnS nanoparticles recorded using an excitation wavelength of 340 nm is shown in figure 5. The figure shows that the as-synthesized ZnS nanoparticles have broad emission band at 445 nm. This blue emission of undoped particles is attributed to self-activated luminescence related to interstitial sulfur ion. Several research groups [21-23] have also reported similar blue emission for ZnS nanoparticles. In Cr doped ZnS samples photoluminescence quenching was observed. The luminescence quenching as a result of Cr doping is attributed to repeated excitations within the Cr sites and thermal escape of charge carriers from confined states to other states. D.A.Reddy et al [24] have observed similar photoluminescence quenching for 3% Cr doped nanoparticles. From PL spectra it is observed that as Cr concentration increases the luminescence intensity decreases this property is attributed towards the formation of deep centers which can inhibit more electrons (holes) to be excited and can lead to the enhancement of nonradiative recombination processes. As a result, their emission intensities become weaker than that of pure ZnS nanoparticles. From the PL spectra it is also found that Cr doped samples exhibited shift with increase in Cr doping concentration and this may be due to slight change in particle size of nanoparticles.

Figure 7 illustrates the magnetization versus applied magnetic field (M-H) curves recorded at room temperature using VSM for undoped and Cr (1.99%, 2.54% and 3.02%) doped ZnS samples. From the figure a typical paramagnetic behavior has been observed in the host ZnS and it is attributed to the absence of unpaired electrons in its 'd' orbital. From the figure it is obvious that Cr doped ZnS samples exhibit a strong ferromagnetic ordering at room temperature. In brief, the observed ferromagnetism in Cr doped ZnS nanoparticles is attributed to the substitution of Cr for Zn, which provides the necessary unpaired spins for ferromagnetism. Thus, the observed ferromagnetism in Cr doped ZnS nanoparticles is attributed to the exchange interaction between localized 'd' spins of the Cr ions and the free delocalized carriers. D.A.Reddy et al [24] have observed ferromagnetism in Cr doped ZnS nanoparticles. From the figure 7 it is clear that all Cr doped ZnS samples of all compositions exhibit hysteresis (M-H loop) at room temperature. XRD studies have not indicated the presence of magnetic phases of  $\text{CrO}_2$  or antiferromagnetic phases  $\text{Cr}_2\text{O}_3$  and  $\text{Cr}_3\text{O}_4$  clusters in the present Cr doped ZnS samples. Absence of extra peaks indicates that there are no other impurities present in the samples. Hence it may be concluded that the observed ferromagnetism in the present samples is not due to the presence of any secondary phases, and is attributed solely to the doping of Cr in ZnS lattice. From the hysteresis loop it is observed that (M-H loop) ferromagnetism is much stronger in 1.99% Cr doped ZnS nanoparticles than 2.54% and 3.02% Cr doped ZnS nanoparticles. This is because as the Cr ions substitute for the Zn ions, the hole concentration due to anion increases, thereby Fermi energy level moves up and the exchange interaction is enhanced leading to enhanced ferromagnetism. From the figure it is seen that as the Cr concentration increases the ferromagnetism is suppressed. With increase in Cr concentration (>1.99%), the Cr atoms come closer to each other and the super exchange interaction between neighboring Cr atoms becomes anti-ferromagnetic in nature. The enhanced anti-ferromagnetic interaction arising from the increased volume fraction of Cr ions suppresses the ferromagnetic ordering when Cr dopant concentration is increased.

The values of coercive field ( $H_c$ ) obtained are 1417.8 G for 1.99% Cr doped ZnS, 1258.3 G for 2.54% Cr doped ZnS and 304.74 G for 3.02% Cr doped ZnS nanoparticles. The corresponding values of saturation magnetization ( $M_s$ ) are  $162.86 \times 10^{-6}$ ,  $303.59 \times 10^{-6}$  and  $371.28 \times 10^{-6} \text{ emu/g}$  for 1.99%, 2.54% and 3.02% Cr doped ZnS nanoparticles. The values of retentivity ( $M_r$ ) are  $81.723 \times 10^{-6}$ ,  $35.504 \times 10^{-6}$  and  $52.809 \times 10^{-6}$  for 1.99%, 2.54% and 3.02% Cr doped ZnS nanoparticles. It is observed that ZnS nanoparticles with lower Cr (1.99%) concentration exhibited strong ferromagnetism, whereas in samples with higher Cr (2.54 and 3.01%) concentration.

Optical absorption spectra of undoped and Cr doped ZnS nanoparticles are shown in Fig 5. It is well known that the position of absorption edge is related to the size of the nanoparticles. The absorption edge of the ZnS nanoparticles shows a blue shift and is located at 300 nm when compared to the value 337 nm of bulk ZnS. This blue shift is due to quantum confinement effect which is due to decrease in particle size [25-26]. Absorption spectra of Cr doped ZnS nanoparticles shows that the absorption edge is slightly shifted towards the longer wavelength (red shift) when compared to undoped ZnS. The shift of the absorption edge to the longer wavelength is due to the small increase of particle size with increasing Cr concentration. The fundamental absorption, which corresponds to the electron excitation from the valance band to the conduction band, can be used to determine the nature and value of the optical band gap. The absorption maxima for undoped and 1.99%, 2.54% and 3.02% Cr doped ZnS nanoparticles lie at 300 nm, 302 nm, 306 nm and 307 nm, respectively. The band gap of all the samples was calculated using a simple wave energy equation [27].

$$E = h \nu = \frac{hc}{\lambda} \text{ ----- (2)}$$

The band gap has been calculated and is found to be 4.14, 4.11, 4.06 and 4.04 eV for undoped ZnS and 1.99% Cr, 2.54% Cr and 3.02% Cr doped ZnS respectively.

In a bulk semiconductor a bound electron – hole pair, called an exciton, can be produced by a photon having an energy greater than that of the band gap of the material. The band gap is the energy separation between the top filled energy level of valance band and nearest unfilled level in the conduction band above it. The photon excites an electron from the filled band to the unfilled band above. The result is a hole in the otherwise filled valance band, which corresponds to an electron with an effective positive charge. Because of the Coulomb attraction between the positive hole and the negative electron, a bound pair, called an exciton, is formed that can move through the lattice. The existence of the exciton has a strong influence on the electronic properties of the semiconductor and its optical absorption. It is particularly interesting to see what happens when the size of the nanoparticles becomes smaller than or comparable to the radius of the orbit of the electron – hole pair. There are two situations, called the weak confinement and the strong confinement regimes. In the weak regime the particles radius is larger than the radius of the electron – hole pair, but the range of motion of the exciton is limited, which causes a blue shift of the absorption spectrum. When the radius of the particle is smaller than the orbital radius of electron – hole pair, the motion of the electron and hole become independent and the exciton does not exist. The hole and electron have their own set of energy levels. Here also there is a blue shift [28]. Quantum size effects become dominating when the size of the nanocrystallites is less than bulk exciton Bohr radius and it affects the electronic energy bands of the semiconductors. Coulomb interaction between the hole and the electron plays a crucial role in nanocrystalline materials. The quantum confinement of charge carriers modifies the valence and conduction bands of the semiconductors. The blue shift in the band gap of nanoparticles due to quantum confinement is of the quantitative form [29]

$$E_g^{nano} = E_g^{bulk} + \frac{\hbar^2 \pi^2}{2\mu R^2} - \frac{1.8e^2}{\epsilon R} \text{ ----- (3)}$$

where  $E_g^{nano}$  and  $E_g^{bulk}$  are the band gap values of the nanoparticles and the bulk material respectively,  $\mu = m_e m_h / (m_e + m_h)$  is the reduced mass and  $m_e$  and  $m_h$  are effective masses of electron (0.19  $m$  for ZnS) in conduction band and holes (0.80  $m$  for ZnS) in valance band respectively,  $e$  is the electron charge,  $\epsilon$  is the relative permittivity of the semiconductor,  $R$  is the radius of the particle and the second term is the columbic term and is generally neglected. The particle size has been calculated using Eq.3. The particle size of ZnS and Cr doped ZnS is found to lie in the range of 4-5 nm. As the particle size obtained from X-ray diffraction, HRTEM and optical absorption studies is smaller than Bohr radius of 2.5 nm for ZnS, the strong confinement effect is assumed to be present in the prepared ZnS and Cr doped ZnS quantum dots.



#### **IV. CONCLUSION**

ZnS and Cr doped ZnS nanoparticles have been prepared by chemical precipitation method. X-ray diffraction results reveal that ZnS and Cr doped ZnS nanoparticles exhibit cubic zincblende structure. The average particle size of the nanoparticles is found to be in the range of 4.8 – 5.2 nm. HRTEM image shows the formation of ZnS and Cr doped ZnS nanoparticles with an average particle size of 4.6 – 5.0 nm. The PL spectra of undoped and Cr doped ZnS samples shows blue emission and a rapid luminescence quenching was observed with increasing Cr concentration. The absorption edge of Cr doped ZnS nanoparticles is found to be shifted towards longer wavelength side when compared to that of undoped ZnS and the band gap is observed to lie in the range of 4.18 – 4.23 eV. The nanoparticles with lower Cr concentration exhibited strong ferromagnetism, whereas in samples with higher Cr concentrations the ferromagnetism was found to be suppressed.

#### **REFERENCES**

- [1.] C. Falcony, M. Garcia, A. Ortiz, J.C. Alonso, J. Appl. Phys. 72 (1992) 1525–1527.
- [2.] M. Bredol, J. Merikhi, J. Mater. Sci. 33 (1998) 471–476.
- [3.] J. Leeb, V. Gebhardt, G. Muller, D. Haarer, D. Su, M. Giersig, G. McMahon, L.
- [4.] Spanhel, J. Phys. Chem. B 103 (1999) 7839–7845.
- [5.] W. Chen, Z. Wang, Z. Lin, L. Lin, Appl. Phys. Lett. 70 (1997) 1465–1467
- [6.] A.P. Alivisatos, Science 271 (1996) 933
- [7.] Qi Xiao, Chong Viao, Applied Surface Science 254 (2008) 6432–6435
- [8.] A. Divya, K. Sivakumar, P. Sreedhara Reddy, Applied Surface Science 258 (2011) 839–842
- [9.] Y. Liu, K. Ai, Q. Yuan, L. Lu, Biomaterials 32 (2011) 1185–1192
- [10.] A.A. Khosic, M. Kundu, L. Jatwa, S.K. Deshpande, U.A. Bhagwat, M. Sastry, S.K. Kulkarni, Appl. Phys. Lett. 67 (1995) 2702–2704.
- [11.] Eugenio Caponetti, Delia Chillura Martino, Maurizio Leone, Lucia Pedone, Maria Luisa Saladino, Valeria Vetri, J. Colloid Int. Sci. 304 (2006) 413–418.
- [12.] Jianling Zhang, Buxing Han, Juncheng Liu, Xiaogang, Gunaying Yang, Huaizhou Zhao, J. Supercrit. Fluids 30 (2004) 89–95.
- [13.] Tianyou Zhai, Zhanjun Gu, Ying Ma, Wensheng Yang, Liyun Zhao, Jiannian Yao, Mater. Chem. Phys. 100 (2006) 281–284.
- [14.] J.T. Siy, M.H. Bart, Chem. Mater. 22 (2010) 5973–5982
- [15.] Q. Mq, J. Chen, X. Wu, P. Wang, Y. Yue, N. Dai, J. Lumin. 131 (2011) 2267–2272
- [16.] Q. Zhao, Y. Xie, Z. Zhang, X. Bai, Cryst. Growth Des. 7 (2007) 153–158
- [17.] H. Li, F. Qu, Chem. Mater. 19 (2007) 4148–4154
- [18.] Hemant Soni, Mukesh Chawda, Dhanajay Bodas, Materials Letters 63 (2009) 767–769
- [19.] H. Wang, Y. He, T. Ji, X. Yan, Anal. Chem. 81 (2009) 1615–1621.
- [20.] Dan Xu, Zhaoping Lu, Jianbo Liang and Yitai Qian, J. Phys. Chem B 109 (2005) 14344–14349
- [21.] B.S.R. Devi, R. Raveendran, A.V. Vaidyan, Pramana, J. Phys. 68 (2007) 679–687.
- [22.] W.G. Becker, A.J. Bard, J. Phys. Chem. 87 (1983) 4888–4893.
- [23.] N. Murase, R. Jaganathan, Y. Kanematsu, M. Watanabe, A. Kurita, H. Hirata, T. Yazawa, T. Kushida, J. Phys. Chem. B 103 (1999) 754–760.
- [24.] S. Yanagida, M. Yoshida, T. Shiragami, C. Pac, H. Mori, H. Fujita, J. Phys. Chem. 94 (1990) 3104–3111.
- [25.] D. Amaranatha Reddy, G. Murali, R.P. Vijayalakshmi, B.K. Reddy, B. Sreedhar, Cryst. Res. Technol. 46 (2011) 731–736.
- [26.] R. Sarkar, C.S. Tiwary, P. Kumbhakar, S. Basu, A.K. Mitra, Physics E. 40 (2008) 3115.
- [27.] A. Sing, M. Limaye, S. Sing, N.P. Lalla, C.K. Malek, S. Kulkarni, Nanotechnology 19 (2008) 245613.
- [28.] G. Murugadoss, Journal of Luminescence 132 (2012) 2043–2048
- [29.] M. Maleki, M. Sasani, Ghamsari, Sh. Mirdamadi, R. Ghasemzadeh, Semiconductor Physics, Quantum Electronics & Optoelectronics, 10 (2007) 30–32.
- [31.] M. Asha Jhonsi, A. Kathiravan, R. Renganathan, Journal of Molecular Structure 921 (2009) 279–284.
- [32.]

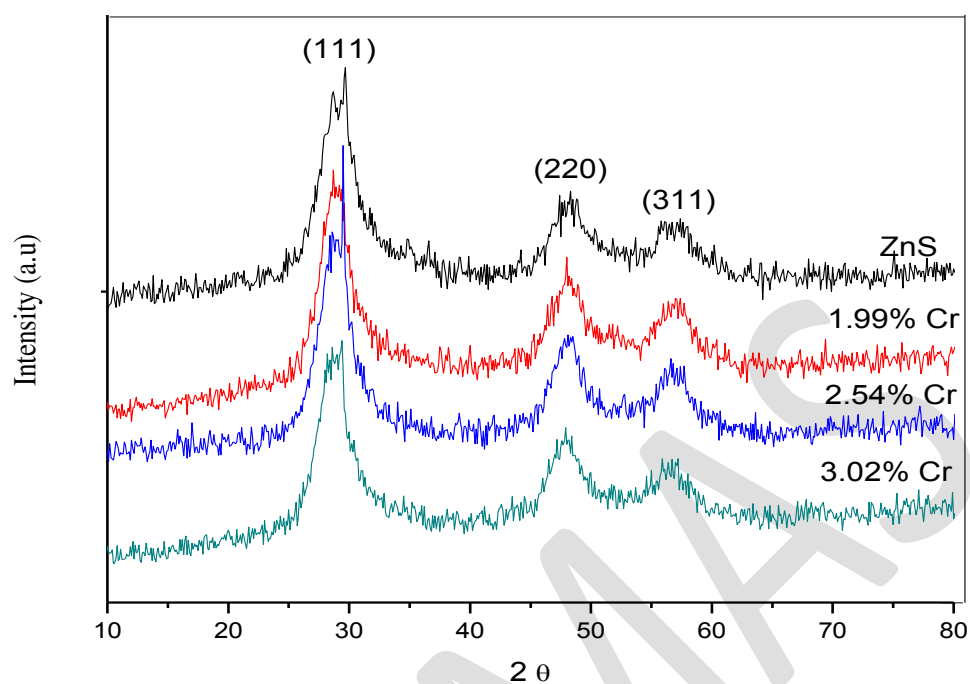


Figure 1. X-ray diffraction pattern of ZnS and Cr doped ZnS

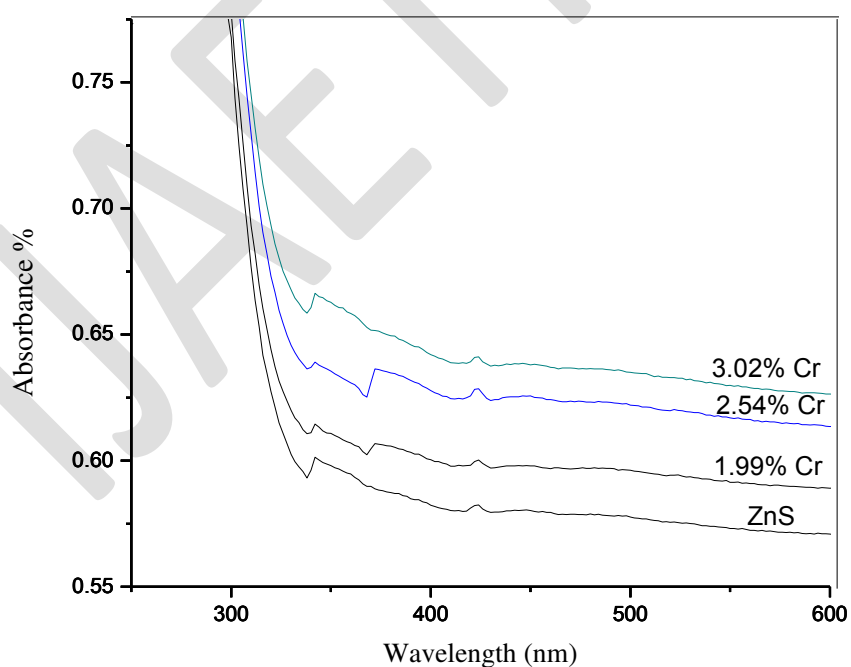


Figure 7. UV Absorbance spectra of ZnS and Cr doped ZnS nanoparticles.

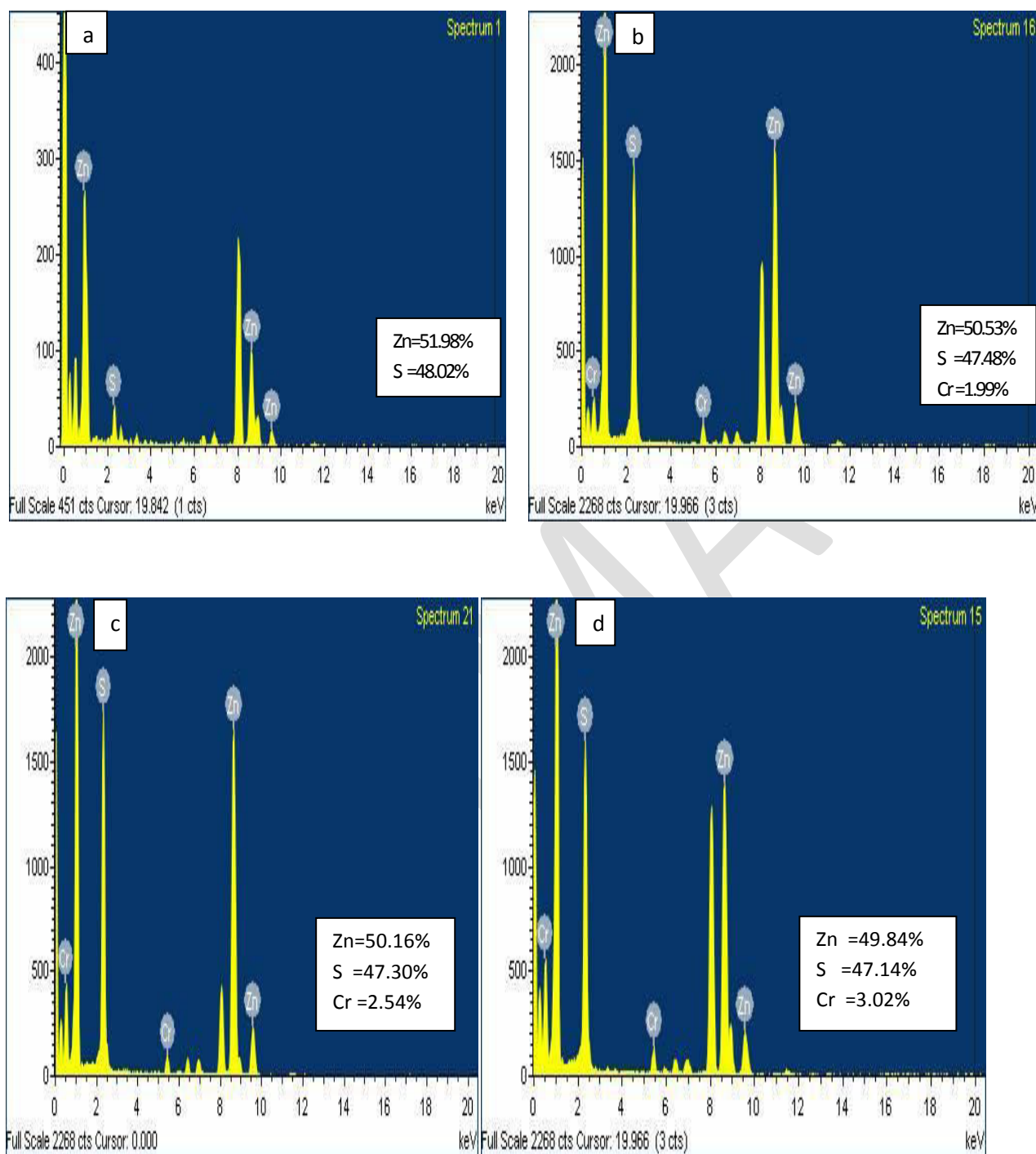


Figure 3. EDAX pattern of ZnS and Cr doped ZnS

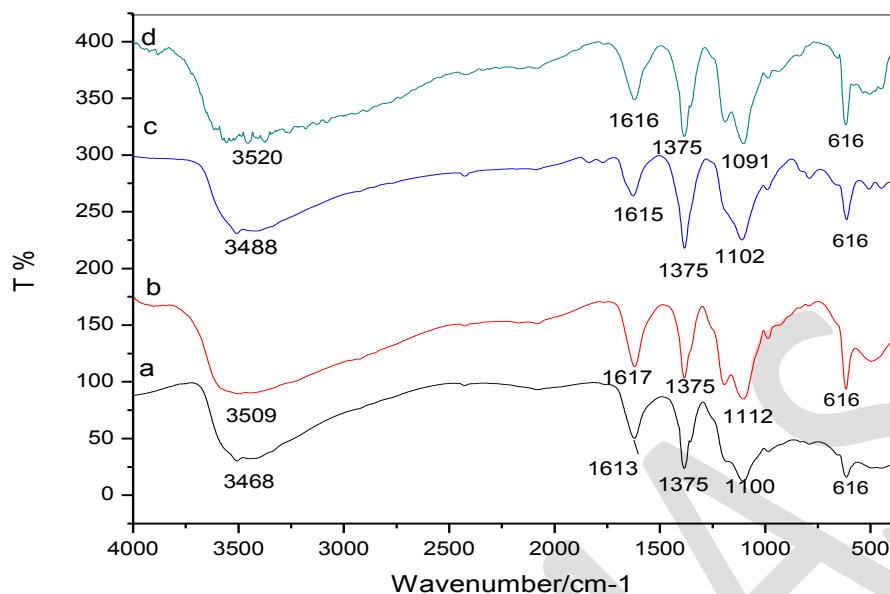


Figure 4. FTIR spectra of (a) ZnS, (b) 1.99% Cr, (c) 2.54% Cr and (d) 3.02% Cr doped ZnS

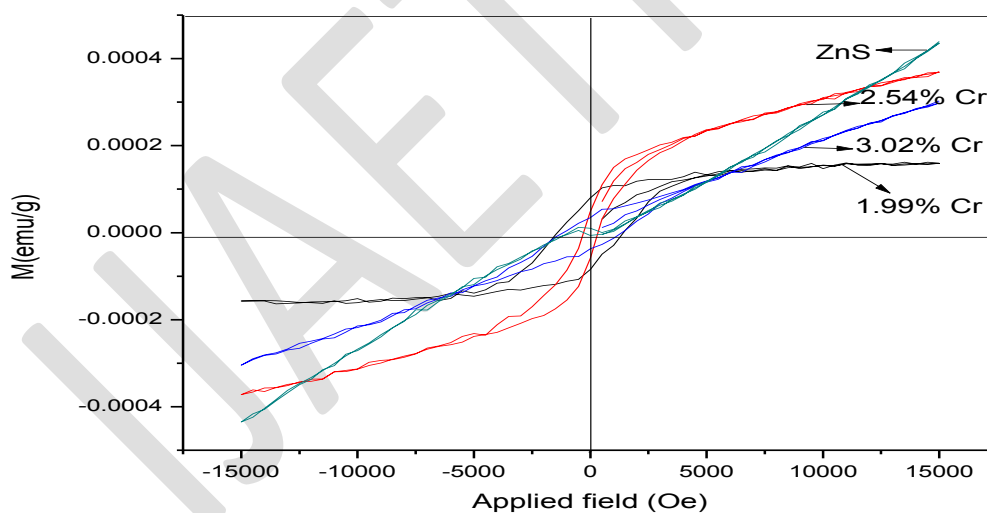


Figure 6. Plot of magnetization versus magnetic field of ZnS and Cr doped ZnS nanoparticles



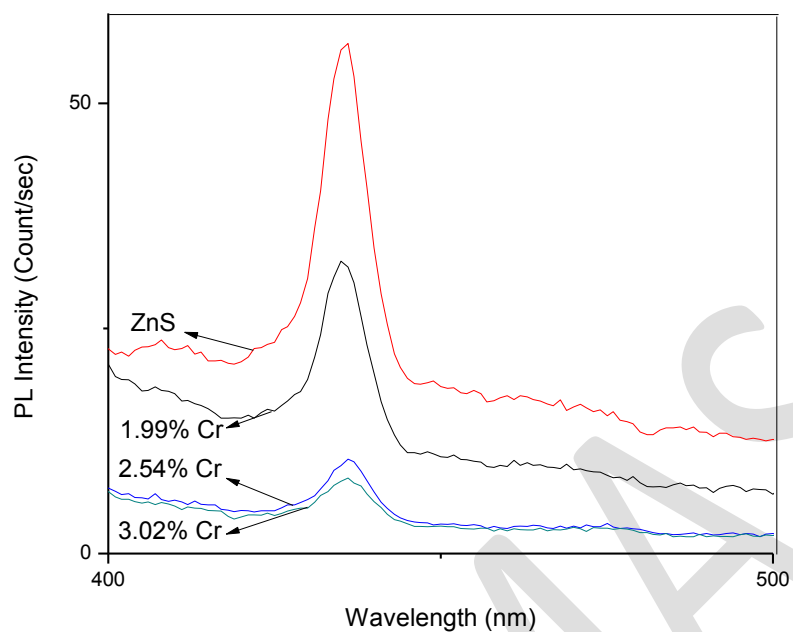


Figure 5. PL emission spectra of ZnS and Cr doped ZnS nanoparticles.

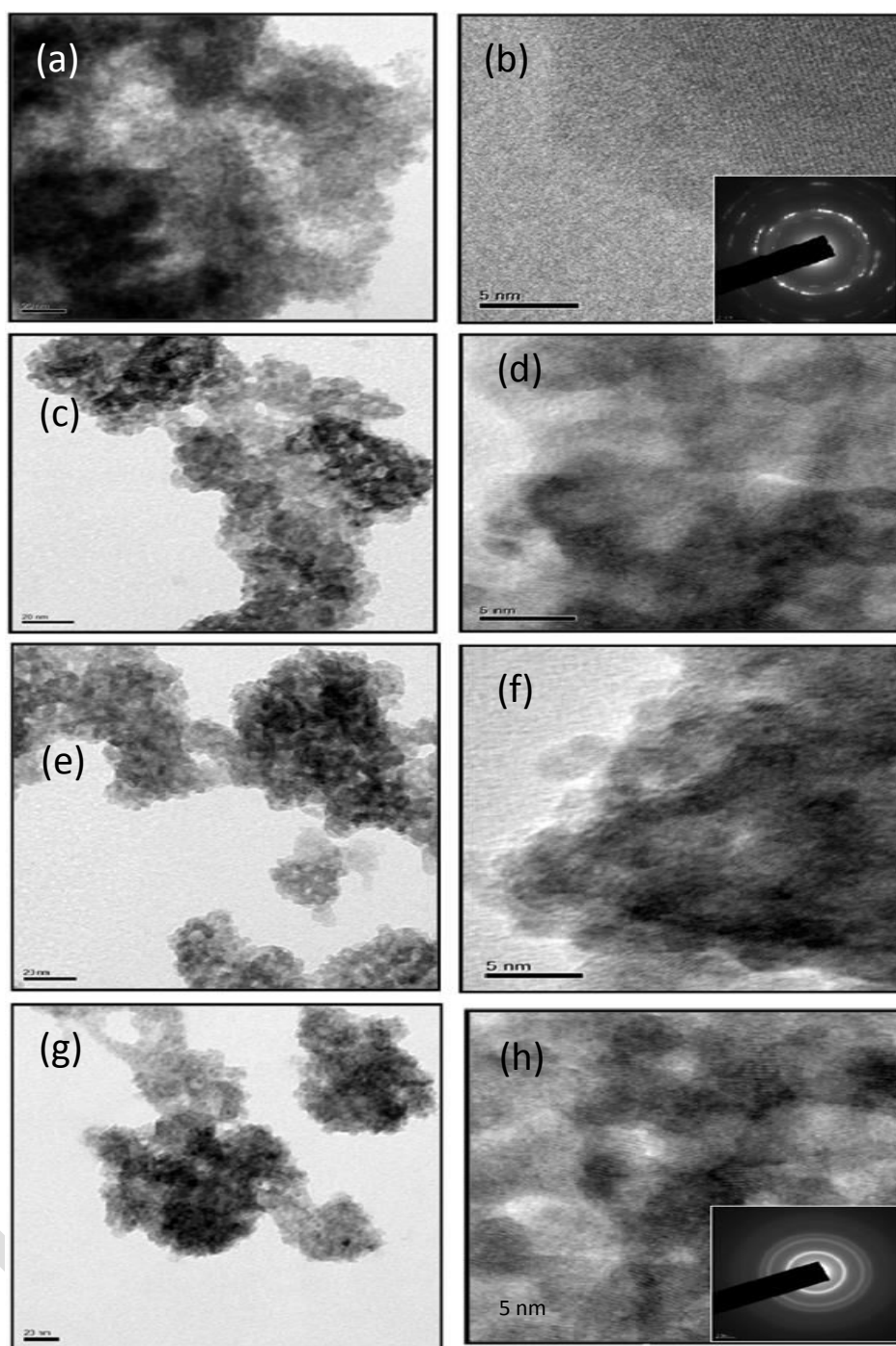


Figure 2.HRTEM images of (a, b) ZnS and Cr doped ZnS, (c, b) 1.99% Cr, (e, f) 2.54% Cr and (g, h) 3.02% Cr

Table 1 Structural parameters of ZnS and Cr doped ZnS nanoparticles

Material	$2\theta_{(111)}$	$d\text{ (\AA)}$	Calculated values	Grain size (nm)
			$a\text{ (\AA)}$	
ZnS	28.69	3.106	5.397	4.8
1.99% Cr doped ZnS	28.80	3.098	5.384	5.0
2.54% Cr doped ZnS	28.85	3.096	5.365	5.1
3.02% Cr doped ZnS	28.94	3.091	5.352	5.2